

See discussions, stats, and author profiles for this publication at: <https://www.researchgate.net/publication/51856528>

Microfabricated Linear Hydrogel Microarray for Single-Nucleotide Polymorphism Detection

ARTICLE *in* ANALYTICAL CHEMISTRY · DECEMBER 2011

Impact Factor: 5.64 · DOI: 10.1021/ac202303f · Source: PubMed

CITATIONS

12

READS

25

5 AUTHORS, INCLUDING:



Erik Jensen

HJ Science & Technology, Inc.

20 PUBLICATIONS 331 CITATIONS

[SEE PROFILE](#)



Jungkyu Kim

Texas Tech University

52 PUBLICATIONS 529 CITATIONS

[SEE PROFILE](#)



Yun Kyung Jung

Ulsan National Institute of Science and Techn...

23 PUBLICATIONS 289 CITATIONS

[SEE PROFILE](#)

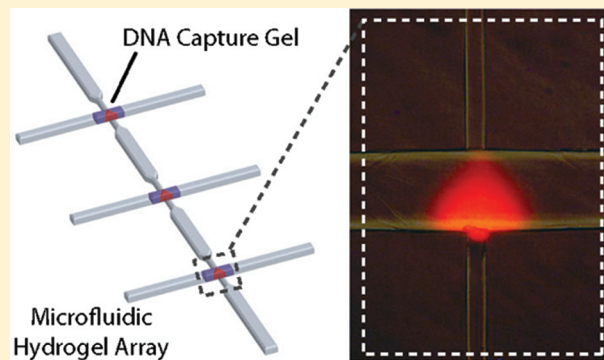
Microfabricated Linear Hydrogel Microarray for Single-Nucleotide Polymorphism Detection

Avraham Bromberg,[†] Erik C. Jensen, Jungkyu Kim, Yun Kyung Jung,[‡] and Richard A. Mathies*

Department of Chemistry, University of California, Berkeley, California 94720, United States

 Supporting Information

ABSTRACT: A platform is developed for rapid, multiplexed detection of single-nucleotide polymorphisms using gels copolymerized with oligonucleotide capture probes in a linear microchannel array. DNA samples are analyzed by electrophoresis through the linear array of gels, each containing 20–40 μM of a unique oligonucleotide capture probe. Electrophoresis of target DNA through the capture sites and the high concentration of capture probes within the gels enables significantly shorter incubation times than standard surface DNA microarrays. These factors also result in a significant concentration of target within the gels, enabling precise analysis of as little as 0.6 femtmoles of DNA target. Differential melting of perfectly matched and mismatched targets from capture probes as a function of electric field and temperature enables rapid, unambiguous identification of single-nucleotide polymorphisms.



The DNA microarrays developed over the last fifteen years have had an enormous impact on genomic analysis,¹ disease diagnosis,^{2–4} drug discovery,⁵ cancer research,⁶ pathogen detection,⁷ forensic analysis,⁸ and pathology research.⁹ Of great interest is the detection of single-nucleotide polymorphisms (SNP) due to their association with cancer and other diseases. Detection of SNPs in highly parallel hybridization assays is exceedingly powerful but can also be challenging due to nonspecific hybridization,^{10,11} as well as detection and hybridization time issues.

The operation of standard microarrays is based on hybridization between a set of known surface immobilized single-stranded DNA (ssDNA) capture probes with fluorescently labeled DNA from an unknown sample. DNA microarrays are composed of tens of thousands to hundreds of thousands of robotically spotted or photolithographically synthesized DNA probes on a glass or silicon wafer.¹² Despite the wide use of these microarrays, this technology has several limitations: (i) the number of probe molecules in a surface element is typically limited to 2.5–12 attomoles per feature size of 25–120 μm^2 ,^{13,14} (ii) diffusion of targets to the probe location takes 16–48 h and is inefficient,¹⁵ (iii) the number of samples analyzed per array can be limited,¹⁶ (iv) relatively large volumes (\sim 100–200 μL) of sample are required,¹⁶ and (v) the sensitivity for expression studies is not high enough to enable analysis without performing PCR.¹⁷

Alternatively, Illumina has developed arrays of microbeads with capture oligonucleotides for genotyping and SNP detection.^{18–21} Although Illumina microarray platforms have sensitivities in the range of subpicmolar to picomolar,²² while the sensitivities of the standard microarrays are in the range of subnanomolar to nanomolar,²³ large (40–60 μL) sample volumes are

still required, and the hybridization process is in the range of 16–20 h.²⁴

Significant improvements in the speed and sensitivity of DNA hybridization have been achieved by immobilizing DNA capture probes within gel matrixes and transporting the target DNA toward the anchored DNA probes by a controlled DC voltage.^{25–27} These 3D hydrogels increase the capacity for trapped DNA probes, enable free movement of the target DNA analytes, and thus provide more favorable binding kinetic conditions than those of the solid liquid interface.²⁸ By applying a DC electric field where the positive electrode was covered by a gel layer containing an immobilized DNA probe, target DNA was concentrated within the gel layer and the hybridization speed was enhanced by a factor of 25–40.^{27,29} Although these devices successfully addressed some of the microarray limitations, the requirement for sophisticated power supplies and the use of semiconductor elements for each test spot on the chip increase costs and fabrication complexity.²⁶ Also, such electrode formats introduce complications due to electrolysis at the probe electrode.

Many of the limitations mentioned above can be addressed by incorporating DNA hybridization procedures into microfluidic electrophoresis lab-on-a-chip systems. Since sample and reagent volumes are reduced, the speed of the process can be increased and costs are reduced.^{30,31} In the past decade, our laboratory has established techniques for the integration of numerous bioassays into microfluidic platforms. We have demonstrated the ability to perform high quality electrophoretic

Received: August 30, 2011

Accepted: December 6, 2011

Published: December 6, 2011



injection and separations in dense arrays of microfabricated capillaries,^{32,33} developed a reliable integrated nanoliter PCR amplification reactor,^{34,35} and developed dense arrays of micro-valves for complex sample processing operations.^{36,37} Recently, methods have also been developed to capture DNA targets in photopolymerized capture gels in microfabricated injectors to purify sequencing fragments in preparation for electrophoretic separations.^{38,39} The latter result leads naturally to the possibility of melding microfluidic and microarray technology.

Here, we develop a method to prepare linear arrays of photopolymerized capture gels in a network of microfluidic channels for high-speed, multiplexed detection and identification of genetic sequences. This system provides high sensitivity and the ability to simultaneously assay multiple targets from a low volume sample. We present a proof of principle study showing that a mixture of three different DNA targets are separated and concentrated in a microfluidic array containing three different photopolymerized DNA capture gels. Additionally, we show that mutations within the trapped target DNA are easily identified by performing rapid melting analysis and comparing the dissociation temperatures (T_d) of capture sequences for mutant and wild type alleles under constant electrophoretic conditions. The high signal-to-noise and specificity of our 3-dimensional DNA capture gel technology enables specific, accurate, and reproducible identification of SNPs in a population of mixed targets.

MATERIALS AND METHODS

Materials. Acrylamide (AA), poly(ethyleneglycol) diacrylate MW 700 (PEGDA), 2-hydroxy-2-methylpropionophenone (HMPP) were obtained from Aldrich, (Milwaukee, WI). Oligonucleotides were purchased from Integrated Technologies (IDT, San Diego, CA) and are listed in Table 1. Capture

Table 1. Complementary and Single-Base Mismatched Capture Oligonucleotides

name	T_m (°C)	sequence ^a
K12probe1	51.5	5'-/5Acryd/CCA GTA ATC ATC GTC TGG AT-3'
K12probe1matchFAM	51.5	5'-/56 FAM/ATC CAG ACG ATG ATT ACT GG-3'
K12probe1misG3FAM	47.1	5'-/56 FAM/ATC CAG ACG ATG ATT <u>ACG</u> GG-3'
K12probe1misG3TEX	47.1	5'-/STEX615/ATC CAG ACG ATG ATT <u>ACG</u> GG-3'
K12probe1misG10TEX	48.9	5'-/STEX615/ATC CAG ACG <u>AGG</u> ATT ACT GG-3'
K12probe1misT15TEX	44.5	5'-/STEX615/ATC <u>CAT</u> ACG ATG ATT ACT GG-3'
K12probe2	53.8	5'-/5Acryd/CCA GTG CTT CGC ATA TTC TG-3'
K12probe2matchFAM	53.8	5'-/56 FAM/CAG AAT ATG CGA AGC ACT GG-3'
K12probe2misT10TEX	46.4	5'-/STEX615/CAG AAT ATG <u>CTA</u> AGC ACT GG-3'
M13mp18	53.6	5'-/5Acryd/ACT GGC CGT CGT TTT ACT A-3'
M13mp18matchFAM	53.6	5'-/56 FAM/TAG TAA AAC GAC GGC CAG T-3'
M13mp18misT10TEX	45.6	5'-/STEX615/TAG TAA AAC <u>TAC</u> GGC CAG T-3'

^aThe location of mismatches are underlined and bold.

oligonucleotides were dissolved in 1× TE buffer (IDT), pH 7.5, to a concentration of 1 mM, and all other sequences were

dissolved in the same buffer to a concentration of 100 μM. Target oligonucleotides in the range of 1–10 nM were prepared by dilution with 1× TE buffer (IDT), pH 8.0. All oligonucleotides were stored at −20 °C. 1× TTE, pH 8.4, was prepared from 50 mM Tris, 50 mM TAPS free acid, and 1 mM EDTA.

Chip Design and Microfabrication. Devices were prepared using conventional photolithography and wet chemical etching of 1.1 mm thick borofloat glass wafers as described previously.⁴⁰ Figure 1 presents the layout of a gel capture array

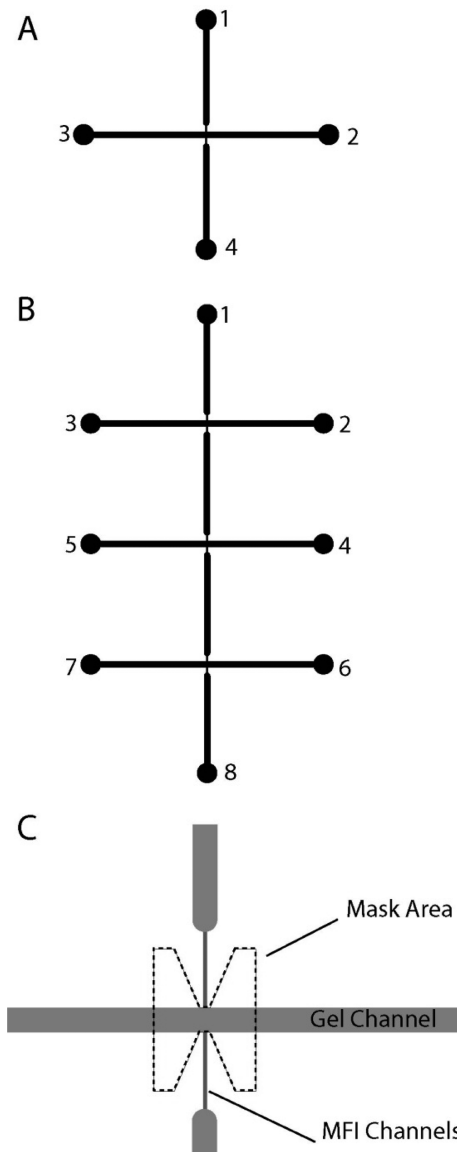


Figure 1. (A) Layout of a single gel capture array unit. Inlet wells are numbered 1–4. A DNA capture gel is photopolymerized within the horizontal gel channel. Samples are electrophoresized through the vertical sample channel which contains microfluidic interface (MFI) units to restrict fluid flow before and during photopolymerization. (B) Design of an array containing three capture gel channels and a single sample channel. (C) Mask structure for a single gel capture array unit used to limit photopolymerization to a small plug at the intersection between the gel and sample channels.

unit. Each unit consists of a horizontal gel channel and vertical sample channel. To prepare gels without cross contamination at the intersection of two microchannels, mixing of the

prepolymerized solutions from the orthogonal channels must be minimized. To minimize such mixing, we incorporated microfluidic interface (MFI) elements at the intersection between the gel and sample channels.⁴⁰ The MFI element is a short channel with a much smaller cross sectional area than that of the two connected microchannels. Each MFI element was 400 μm long, 25 μm wide, and 10 μm deep. The 50 μm wide electrophoresis channels were etched to a depth of 30 μm . The 150 μm wide gel channels were etched to a depth of 30 μm . The overall length of the gel and sample channels shown in Figure 1A is 10 mm. Figure 1B shows the layout of an array containing three DNA capture gel channels. The length of each gel channel is also 10 mm, while the length of the sample channel of Figure 1B is 20 mm.

Gel Preparation. The cross-linked DNA affinity capture gel in the microchannel intersection zone was prepared *in situ* by photopolymerizing cross-linked acrylamide with 5'-acrydite-modified oligonucleotide capture probes similar to a procedure published earlier.³⁵ However, a nonfluorescent photoinitiator, 2-hydroxy-2-methyl-1-phenyl propanone (HMPP),⁴¹ was chosen instead of the fluorescent photoinitiator riboflavin in order to obtain a nonfluorescent background. Photopolymerization with HMPP can be carried out under nitrogen atmosphere.

Gels in a single intersection of the microchannel structure were prepared according to the following procedure. Two prepolymer solutions were prepared composed of (w/v): 5% AA, 0.5% cross-linker polyethylene glycol diacrylate (PEGDA), 0.007% photoinitiator HMPP, 1× TTE, and one of the solutions also contained 20 or 40 μM 5'-acrydite-modified DNA probe. The solution mixtures were sparged with N₂ for 30 min. The device was placed under the objective of an inverted Zeiss Axioskop microscope positioned in a glovebox which was then flushed with nitrogen for 30 min. Each device was loaded with prepolymer solution without DNA probe in the sample channel and prepolymer solution containing DNA probe in the gel channels. After solution loading, the chip was aligned with the designed mask prepared for restricted area exposure (see Figure 1C). A vacuum chuck attached on the microscope stage held the mask and the wafer in place. The chip was illuminated through the chrome mask from the bottom of the wafer for 6 min by a 100 W mercury lamp with a UV filter that transmitted light in the region 330–365 nm and power of 10 mW/cm². After photopolymerization was completed, the unpolymerized acrylamide monomers and oligonucleotides were washed out from the sample channel by electrophoresis for 10 min under field strength of 40 V/cm. The procedure for gel preparation in the array containing three DNA gel channels (Figure 1B) was slightly modified. Three different capture gels containing M13mp18, K12probe1, and K12probe2 were prepared within the channels of the multiplexed gel capture device. A detailed description of these procedures can be found in the Supporting Information section.

DNA Capture. Once the capture gels were formed within the intersections of the microchannels, the chip was placed on a 2 × 2 × 0.25 in. temperature controlled aluminum block for sample loading by electrophoresis. To create good thermal contact between the glass chip and the aluminum block, a thin layer of water-soluble heat sink compound was used as an interface between the two surfaces. For temperature calibration, a 500 μm diameter hole was drilled 5 mm into the side of the chip and a thin thermocouple was inserted for comparison to the temperature of the aluminum block. Samples containing fluorescently labeled oligonucleotides were placed in well 1 of Figure 1A or 1B, and a constant field of 40 V/cm between well

1 to well 4 or 8 drove the oligonucleotides through the capture gels. Detectable capture of DNA sample was obtained after 10 min electrophoresis in a single gel and 20–30 min electrophoresis in the array of three gels. Residual DNA within the channels was washed out by 10 min electrophoresis under field of 40 V/cm. Epifluorescence images of the gels were acquired using a microscope (Nikon Eclipse E800, objective $\times 20/0.45$), equipped with a set of filters to monitor fluorescence of FAM and Texas Red. Equal initial signals of FAM and Texas Red probes for comparative studies were obtained by adjusting the exposure time of the CCD camera.

The dissociation profile under electrophoretic flow was determined by stepwise heating of the aluminum block to higher temperatures and then electrophoretically washing with buffer for 5 min under field strength of 20–60 V/cm. The dissociation temperature (T_d) is the temperature at which half of the initial trapped target is washed out. It is analogous to the melting temperature (T_m) that is determined under equilibrium conditions but will depend on the applied working voltage.

Data Analysis. Melting temperatures (T_m) of oligonucleotides listed in Table 1 were calculated by IDT software (www.idtdna.com). Free energy changes ΔG^0 were calculated according to published parameters.⁴² The apparent dissociation rate constant k_{ad} may be evaluated for each temperature of the dissociation curve assuming a first order decay. Following the procedure published by others,⁴³ the apparent dissociation rate constant may be calculated using the following equation:

$$k_{ad} = (\ln I_0 - \ln I)/(t - t_0) \quad (1)$$

where I_0 is the intensity before electrophoretic washing, I is the intensity after washing, and $(t - t_0)$ is the time of washing. Since the dissociation rate constant is governed by the thermal dissociation constant k_{td} and by the electric force that may be presented by a rate constant k_{ed} that is proportional to the electric field (E), then $k_{ed} = \alpha E$, where α is a proportional factor. The overall dissociation rate constant is calculated as:

$$k_{ad} = k_{td} + \alpha E \quad (2)$$

From the dependence of k_{ad} on E , k_{td} may be determined.

RESULTS

Successful multiplexed DNA capture depends on the ability to prepare sequence specific capture gels within intersections of orthogonal microchannels in the gel capture array. Successful gel formation was achieved using the MFI elements to prevent significant mixing of the solutions between orthogonal channels and to minimize cross contamination. We prepared gels in intersections of DNA capture gel channels with widths of 100, 150, and 200 μm . The 200 μm channel was too wide, resulting in a large drop of the local field strength relative to the more narrow microchannels. The 100 μm capillary was more difficult to clean and to remove the gels after experiments. We found that 150 μm was the most practical for carrying out experiments, since most of the capture occurred within the initial 30–50 μm of the gel plugs.

Figure 2 presents typical epifluorescence images of the matched oligonucleotide K12probe1matchFAM and the one base mismatched oligonucleotide K12probe1misG3FAM captured by two different capture gels containing K12probe1. DNA capture occurred during electrophoresis for ten min under a field strength of 40 V/cm at 42 °C. A subsequent washing step was

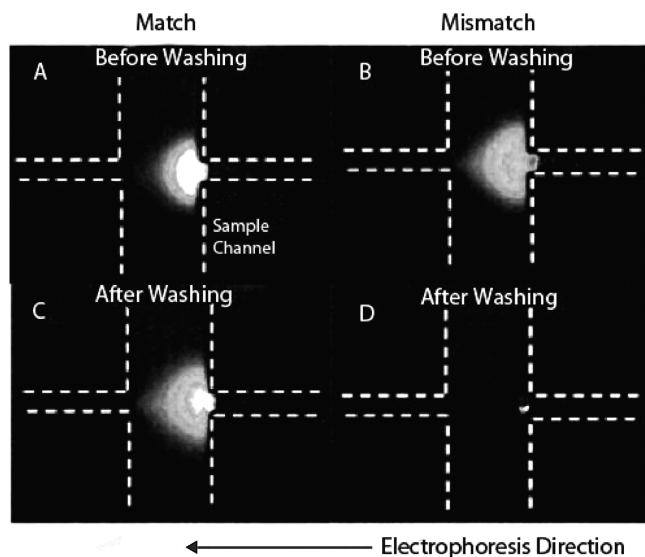


Figure 2. Fluorescence images of captured oligonucleotides on two different gels containing $20\ \mu\text{M}$ capture DNA K12probe1. Sample was loaded and electrophorized for 10 min at a field strength $40\ \text{V}/\text{cm}$ at $42\ ^\circ\text{C}$. Images of the trapped $1\ \text{nM}$ K12probe1matchFAM (A) and of the trapped K12probe1misG3FAM (B) sequences acquired after loading. A subsequent washing step was performed by electrophoresis for 10 min with $1\times$ TTE buffer at $50\ ^\circ\text{C}$ resulting in little decrease in signal for the matched sequence (C) and significantly decreased signal for the mismatched sequence (D).

performed with buffer ($1\times$ TTE pH 8.4) in the inlet for 10 min under the same field strength at $50\ ^\circ\text{C}$.

Due to the high concentration of capture probes in each 3D capture gel, the hybridization process is much faster than capture by oligonucleotides immobilized on a surface. The capture efficiency depends on the association rate constants, thermal dissociation rate constants, electromigration flow, temperature, and electric field strength and distribution. Figure 2 shows that although the two oligonucleotides were both efficiently trapped in the gel at $42\ ^\circ\text{C}$, the mismatch oligonucleotide melted off

when it was washed at $50\ ^\circ\text{C}$ due to the electrophoretic flow and instability of the mismatched base pairs, while a significant signal from the matched sequence is still observed. This process eliminates the interference of mismatched oligonucleotides having weaker interactions with the capture gel, enabling discrimination of matched target from the nonspecifically bound sequences. With no applied electric field, the dissociation of the hybrid is governed by the thermal rate constant; however, under electric field, the dissociation is field strength dependent. By optimizing the field strength and temperature, it is possible to discriminate a single-base mismatched oligonucleotide from the corresponded matched sequence. This ability to tune the melting process with two independent parameters is useful for array design.

The thermal stability of the hybrid complex is characterized by its dissociation temperature T_d . To experimentally determine the dissociation profile of the oligonucleotides trapped in gels under electrophoretic flow, we compared the thermal behavior of a matched oligonucleotide labeled with FAM and a single-base mismatched oligonucleotide labeled with Texas Red. Dissociation curves were obtained for DNA capture gels containing $20\ \mu\text{M}$ K12probe1 at three different field strengths. The sample contained a mixture of K12probe1matchFAM and K12probe1misG3TEX at equimolar concentration ($5\ \text{nM}$). The mismatch oligonucleotide contains a T → G substitution at position 3. (See Table 1.) The two labeled oligonucleotides were simultaneously captured on the same gel by electrophoresis for 10 min at room temperature under an applied voltage of $40\ \text{V}/\text{cm}$. In subsequent washing steps, different field strengths were applied with $1\times$ TTE buffer in the inlet for 5 min at the indicated elevated temperatures. Epifluorescence images of the gels were acquired after stepwise adjustment of temperature during the heating and washing step.

In Figure 3, typical images of the captured matched and mismatched oligonucleotides under three different field strengths (20 , 40 , and $60\ \text{V}/\text{cm}$) and the dissociation curves are presented. Several experiments were carried out for each of the three field strengths, and the evaluated dissociation temperatures are summarized in Table 2. As expected, ΔT_d between

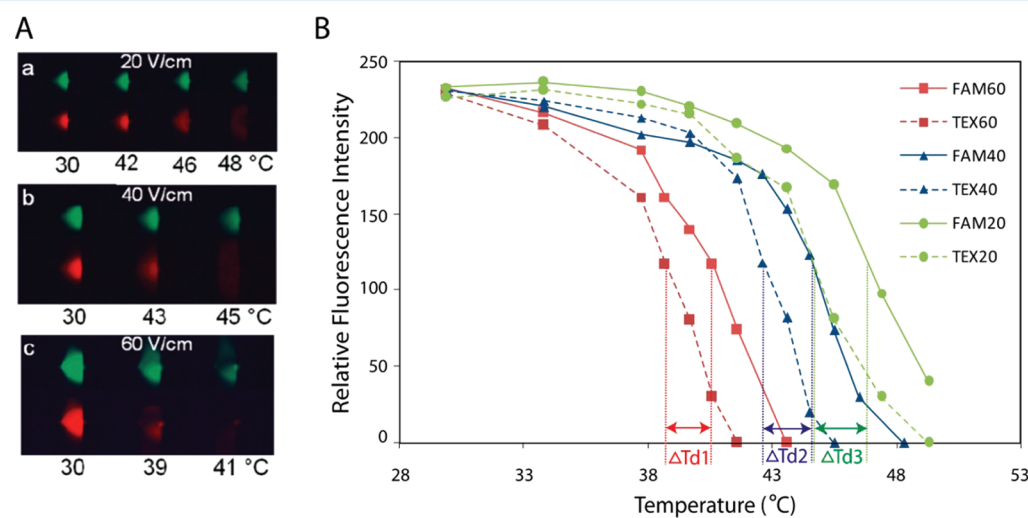


Figure 3. Fluorescence images of K12probe1matchFAM and K12probe1misG3TEX, simultaneously captured and then electrophoretically washed from the same gel. (A) Capture of a mixture of target DNA oligonucleotides was performed at $30\ ^\circ\text{C}$ within a gel containing $20\ \mu\text{M}$ K12probe1 by electrophoresis for 10 min. The captured targets were then washed with $1\times$ TTE buffer at elevated temperatures under three different field strengths as follows: (a) $20\ \text{V}/\text{cm}$, (b) $40\ \text{V}/\text{cm}$, and (c) $60\ \text{V}/\text{cm}$. (B) Typical dissociation curves of K12probe1matchFAM (solid line) and of K12probe1misG3TEX (broken line) under three different field strengths: $20\ \text{V}/\text{cm}$ (green), $40\ \text{V}/\text{cm}$ (blue), and $60\ \text{V}/\text{cm}$ (red) are presented. ΔT_d values (indicated by horizontal arrows) for the three applied voltages were $\Delta T_{d1} = 1.5 \pm 0.7\ ^\circ\text{C}$, $\Delta T_{d2} = 2.1 \pm 0.5\ ^\circ\text{C}$, and $\Delta T_{d3} = 3.1 \pm 0.7\ ^\circ\text{C}$, respectively.

Table 2. Mean Dissociation Temperatures for K12 Hybrids^a

ΔV , V/cm	<i>n</i>	K12probe1matchFAM T_d , °C	K12probe1misG3TEX T_d , °C	ΔT_d , °C
20	5	47.4 ± 1.4	44.3 ± 1.0	3.1 ± 0.7
40	10	44.7 ± 0.9	42.6 ± 0.8	2.1 ± 0.5
60	5	41.5 ± 1.7	40.0 ± 1.4	1.5 ± 0.7

^a T_d values for hybrids of K12probe1 with K12probe1misG3TEX and K12probe1matchFAM were determined by electrophoresis with three different field strengths; *n* = number of experiments.

the dissociation temperatures of the matched sequence and of the single-base mismatched sequence decreased as the field strength increased. At 60 V/cm, some of the gels collapsed due to the high field strength. Although at 20 V/cm the ΔT_d is larger than at 40 V/cm, the slope of the dissociation curves at 20 V/cm is smaller which results in a similar signal ratio of match to mismatch sequences at the T_d for both the 20 and 40 V/cm conditions. Considering runtime, it was concluded that 40 V/cm is a more optimal running condition. The apparent dissociation rate constants are obtained from the dissociation curves for each washing step using eq 1. We estimated the rate constants at 42.6 and 43.5 °C under 20 and 40 V/cm. At the interpolated temperature of 43 °C, the rate constants for matched sequence were: k_{ad} (match) = $(3.8 \pm 1.1) \times 10^{-4} \text{ s}^{-1}$ and $(5.6 \pm 1.4) \times 10^{-4} \text{ s}^{-1}$ under field strength of 20 and 40 V/cm, respectively. Under the same conditions, the rate constants for the mismatched sequence were k_{ad} (mismatch) = $(10.7 \pm 3) \times 10^{-4} \text{ s}^{-1}$ and $(16.9 \pm 4) \times 10^{-4} \text{ s}^{-1}$. Using eq 2, we obtained the dissociation rate constant k_{td} for the match hybrid ($2.0 \times 10^{-4} \text{ s}^{-1}$) and for the mismatch hybrid ($4.5 \times 10^{-4} \text{ s}^{-1}$) at 43 ± 0.5 °C. The evaluated thermal dissociation rate constants are in the range of values obtained for similar oligonucleotides.^{44–46}

The binding energy of double-stranded DNA depends significantly on the position of the composing base pairs.^{23,47} Base pairs in the center typically contribute more significantly to binding energy than base pairs in the vicinity of the end of the strand. However, base composition and base sequence should be also considered.⁴² We examined the T_d of mismatch oligonucleotides of the K12probe1 at three different positions: 3, 10, and 15 from the 3' edge. The obtained T_d values are summarized in Table 3. We observe that the T_d of the duplex with

Table 3. Mean ΔT_d Values for K12probe1 Containing Various Mutations

mutation position	<i>n</i>	experiment T_d , °C	calculated ΔT_m , °C ^a	experiment ΔT_d , °C ^b
none	10	44.7 ± 0.9		
3	10	42.6 ± 0.8	4.4	2.1 ± 0.9
10	4	44.0 ± 0.5	2.6	0.7 ± 0.9
15	4	35.8 ± 0.5	7.0	8.9 ± 0.9

^aDifference between calculated match T_m and that of the mismatch.

^bDifference between experimental match T_d and that of the mismatch; *n* = number of experiments.

the mismatch pair at position 10 is the highest out of the three nucleotides. The order of the experimental T_d values is also supported by calculated values of T_m . Since two (position 3, 10) of the three studied duplexes have the same mismatch pair, we conclude that the differences of the T_d values are a result of the nearest neighbor effect. The parameters compiled by SantaLucia⁴² enable examining the contribution of nearest base pairs at the three different positions to the overall stability

of the three duplexes. At position 3, the neighbor base pairs CA/GG and AG/GC decrease the free energy ΔG^0 by 3.22 kcal/mol relative to the free energy of the match duplex; at position 10, the base pairs CA/GG and AT/GA decrease the free energy ΔG^0 by only 2.24 kcal/mol, while at the position 15 the base pairs TC/AT and CT/TA decrease the ΔG^0 by 4.26 kcal/mol. These results demonstrate that the nearest neighbor effect can be stronger than the position effect.

To explore the feasibility of detecting multiple targets in an array of capture gels, we utilized the device design illustrated in Figure 1B. Three DNA samples were prepared. Each sample was a mixture of 10 nM matched DNA and 10 nM mismatched DNA. The compositions of the samples were as follows:

Sample 1 – K12probe1matchFAM

+ K12probe1misG10TEX

Sample 2 – K12probe2matchFAM

+ K12probe2misT10TEX

Sample 3 – M13mp18matchFAM

+ M13mp18misT10TEX

Sample 1 (6 μL) was driven twice into gel A by electrophoretic flow (40 V/cm) for 20 min at room temperature. The increased loading was done to check whether there is some trapping of the DNA target within the incorrect gels. The gels were washed by electrophoresis with 1× TTE buffer for 15 min, also at room temperature. Samples 2 and then 3 were then serially added to the array using a similar procedure, and the entire experiment was performed in duplicate. In Figure 4, images of the three trapped matched targets (green images) and the corresponding mismatched DNA (red images) of one of the experiments are shown. These data indicated that the DNA in sample 3 passed through gels A and B during the electrophoresis step and was only captured in gel C. Similarly, sample 2 passed through gel A and was only trapped at gel B. Nonspecific interactions were not observed between target sequences and noncomplementary probes. Furthermore, extension of the gel capture technology to a multiplex array did not require significantly longer electrophoretic runtimes. This indicates that the runtime of the system will scale well with the number of target probes.

Similarly, three experiments were performed with a single sample consisting of a mixture of all the six nucleotides (Figure 5). Six microliters of sample volume was loaded into the three capture gel by electrophoresis for 30 min under field of 40 V/cm at room temperature. The chip was heated and electrophoresized with 1× TTE buffer for 5 min at several elevated temperatures. Images of one of the experiments and the dissociation curves for the six oligonucleotides are also presented in Figure 5. This experiment demonstrates that SNP detection by differential mobility of targets within capture gels and dissociation melting curve analysis can be extended to a multiplexed array format.

Although it was not possible to accurately evaluate the T_d values from the curves of Figure 5 because the temperature intervals were relatively large, it is evident that there is a significant difference between the signal intensity of the matched and mismatched oligonucleotides at most temperatures. We can therefore use the gel capture array technology for multiplexed detection of SNPs significantly more rapidly than traditional microarray platforms.

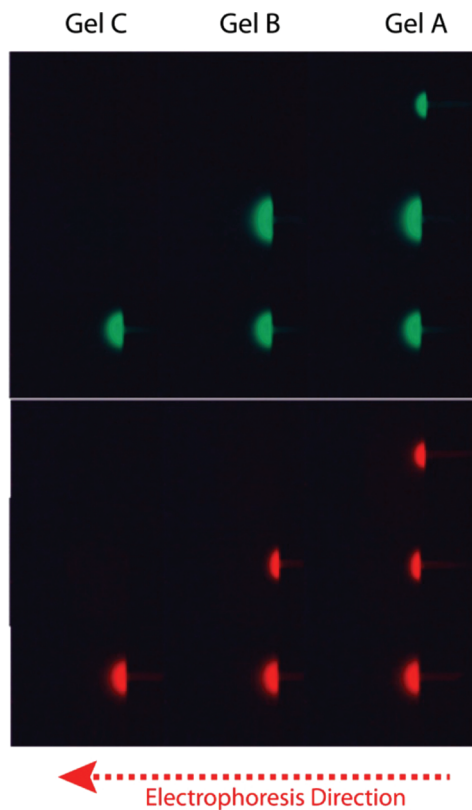


Figure 4. Epifluorescence images of three different trapped match DNA (green) and trapped mismatch DNA (red) samples in a multiplex gel capture array. Gels A, B, and C contain 40 μ M K12probe1, K12probe2, and M13mp18, respectively. Samples 1, 2, and 3 contained 10 nM K12probe1FAM/K12probe1mis10TEX, 10 nM K12probe2matchFAM/K12probe2mis10TEX, and 10 nM M13mp18matchFAM/M13mp18misT10TEX. The samples were loaded at 40 V/cm for 20 min at room temperature. DNA targets pass through elements of the gel capture array if they lack significant complementarity and are trapped at the downstream sequence specific capture sites. Gels were washed before image acquisition.

■ DISCUSSION

We have demonstrated that nonfluorescent capture gels can be formed within the intersection of two microchannels and scaled to linear arrays for SNP detection. Polymerization of DNA capture probes within these gels enables quantitative capture, purification, and concentration of specific gene sequences by electrophoresis. As little as 0.6 femtomoles (2 μ L sample of 0.3 nM concentration) of a 20 basepair oligonucleotide can be trapped and detected with a standard epifluorescent microscope using this technology. This LOD is lower than the value of 10 femtomoles (5 μ L sample of 0.5 nM concentration) obtained by driving DNA target toward a microfabricated electrode coated with a gel layer containing an immobilized DNA trap^{26,29} or 20 femtomoles (50 μ L sample of 0.4 nM) obtained using optical waveguides.⁴⁸ The sample volume required for DNA analysis using a microarray such as the Affymetrix Genome-Wide Human SNP microarray is 200 μ L¹⁶ at a concentration of 0.1–10 nM, corresponding to 20–200 femtomoles²³ of each target. Our results are higher than those obtained by the Illumina bead arrays, ~5.2 attomoles (40 μ L sample of 0.13 pM).²² However, the use of a confocal scanning detection system rather than the simple epifluorescence microscope used here would significantly improve the sensitivity of our assay.

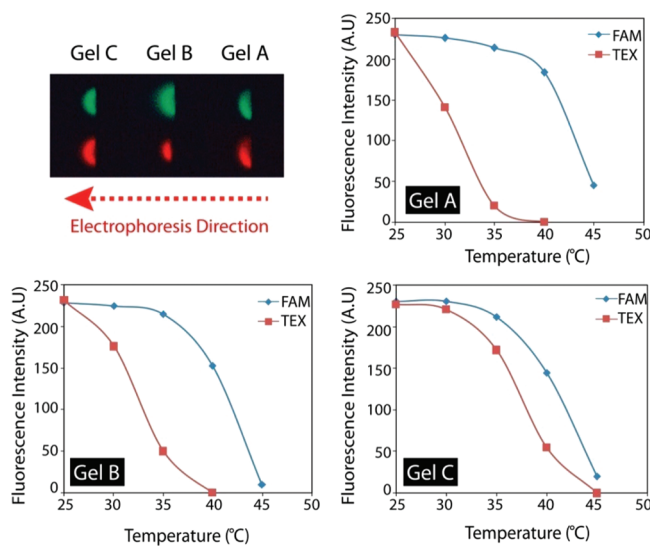


Figure 5. (Top) Fluorescence images obtained from a mixture of 10 nM of all 6 oligonucleotides loaded into the linear capture array of three gels (A, B, and C) by electrophoresis at room temperature for 30 min under field strength of 40 V/cm. Green spots correspond to matched DNA, and red spots correspond to mismatched DNA. After capture, gels were electrophoretically washed at 40 V/cm with 1× TTE buffer for 10 min at each of the several elevated temperatures. Typical dissociation curves for gels A, B, and C demonstrate the successful detection of SNPs in the multiplexed gel capture array.

The shortened hybridization time in our study relative to duplex formation on a glass surface chip is due to the combined use of gels and the electrophoretic transport of targets toward the capture zone. It has been shown that hybridization kinetics within a gel-based microarray can be slower than that of a surface microarray.⁴⁹ However, greater signal is achieved more rapidly in our format due to a larger binding capacity and improved transport properties. A three-dimensional gel provides at least 100 times greater capacity for immobilization than a two-dimensional glass support.³⁰ Furthermore, since diffusion-driven hybridization in dilute solutions under static conditions is very slow, we improve the kinetics by concentrating the target in the gel via electrophoresis.⁴⁹

Using our platform, DNA samples driven by an electric field through the capture gels were characterized according to their binding strength to the matrix as a function of temperature which is reflected by their T_d values. The determined T_d values correlate with the calculated T_m values, although there is a difference between the numeric values mainly because the T_m is calculated for equilibrium conditions while T_d values are determined at nonequilibrium conditions due to the electrophoretic contribution to the dissociation rate. However, the two parameters have the same trend, as the order of the T_d values is the same as that of the T_m values. Therefore, the calculated T_m is a useful parameter for the design of optimal DNA probes for use as a trap in the gel platform. The experimental T_d can be used as a final parameter for selection of the optimal capture oligonucleotide to discriminate the matched oligonucleotide from the mismatched one.

We have also achieved multiplexed detection of DNA targets and SNP identification using an array of capture gels. This one channel array with three intersections enabled demonstration of a multiplexed detection of mutant and wild type alleles from three DNA targets. Nonspecific interaction was not observed between target sequences and noncomplementary probes

because only allele-specific hybridization between probe DNA in hydrogel and target sequence remains within our microfluidic channel under electrophoretic flow conditions.

It should also be possible to identify heterozygous clinical samples using PCR amplification and the methods described here. Amplicons can be generated from clinical samples with two different dyes for mutant and wildtype alleles using fluorescently labeled allele specific primer extension.⁵⁰ Comparison of the two melting curves using capture gel technology would easily enable identification of each genotype. Alternatively, it should be possible to identify heterozygous samples using a single dye labeled amplification product. Since a heterozygous sample would result in an equal mixture of mutant and wildtype amplicons, we expect the melting profile to be a superposition of the mutant melting profile and wildtype melting profile. Although we have used 20 basepair synthetic oligonucleotides for the present work, we previously demonstrated that photopolymerized gels can be used for allele specific capture of variously sized oligonucleotides and PCR products.³⁹

In summary, we have demonstrated 3D microgel array technology with significantly shorter incubation times than standard genetic microarrays. In addition, small sample volumes with low concentrations of target DNA can be used as input in our format due to the concentration effect of the μM scale capture probe in the gel. These properties of 3D gels offer significant advantages over surface arrays. Further optimization of the capture process in combination with signal amplification and/or improved detection techniques may enable rapid genetic microarray analysis without the requirement of front end target amplification. We have previously shown that our gel capture technology can be used to quantitatively capture double-stranded DNA targets³⁹ with a high degree of specificity. Future work will explore the use of double-stranded DNA targets as inputs for the gel capture array and expansion of the array to larger sets of targets. Further geometrical optimization is essential to increase the number of targets and samples that can be assayed on one chip.

The results presented in the present context enable new approaches to rapid multiplexed detection of SNPs in a point of care setting with fully integrated microfluidic sample processing. By coupling on-chip PCR reactors or isothermal amplification methods with photopolymerized capture gels for specific capture, concentration, and purification of amplicons,³⁵ it should be possible to integrate nucleic acid amplification with gel capture array technology for rapid SNP detection.

ASSOCIATED CONTENT

Supporting Information

Additional information as noted in text. This material is available free of charge via the Internet at <http://pubs.acs.org>.

AUTHOR INFORMATION

Corresponding Author

*Phone: (510) 642-4192. Fax: (510) 642-3599. E-mail: ramathies@berkeley.edu.

Present Addresses

[†]Semorex Technologies Ltd., Science Park, Ness Ziona, Israel.

[‡]Korea Advanced Institute of Science and Technology, Daejeon, Korea.

ACKNOWLEDGMENTS

We gratefully acknowledge the previous work of Charles Emrich on the MFI structure. Funding for this work was provided by Samsung Corporation.

REFERENCES

- (1) Chee, M.; Yang, R.; Hubbell, E.; Berno, A.; Huang, X. C.; Stern, D.; Winkler, J.; Lockhart, D. J.; Morris, M. S.; Fodor, S. P. *A Science* **1996**, *274*, 610–614.
- (2) Quackenbush, J. *N. Eng. J. Med.* **2006**, *354*, 2463–2472.
- (3) Housman, D.; Ledley, F. D. *Nat. Biotechnol.* **1998**, *16*, 492–493.
- (4) Collins, F. S.; Guyer, M. S.; Chakravarti, A. *Science* **1997**, *278*, 1580–1581.
- (5) Wang, S.; Cheng, Q. *Methods Mol. Biol.* **1998**, *316*, 49–65.
- (6) Perou, C. M.; Sorlie, T.; Eisen, M. B.; van de Rijn, M.; Jeffrey, S. S.; Rees, C. A.; Pollack, J. R.; Ross, D. T.; Johnsen, H.; Akslen, L. A.; Fluge, O.; Pergamenschikov, A.; Williams, C.; Zhu, S. X.; Lonning, P. E.; Borresen-Dale, A.-L.; Brown, P. O.; Botstein, D. *Nature* **2000**, *406*, 747–752.
- (7) Call, D. R. *Crit. Rev. Microbiol.* **2005**, *31*, 91–99.
- (8) Jobling, M. A.; Gill, P. *Nat. Rev. Genet.* **2004**, *5*, 739–751.
- (9) Pollack, J. R. *Am. J. Pathol.* **2007**, *171*, 375–385.
- (10) Binder, H.; Preibisch, S.; Kirsten, T. *Langmuir* **2005**, *21*, 9287–9302.
- (11) Naef, F.; Lim, D. A.; Patil, N.; Magnasco, M. *Phys. Rev. E* **2002**, *65*, 040902.
- (12) Heller, M. J. *Annu. Rev. Biomed. Eng.* **2002**, *4*, 129–153.
- (13) Gunderson, K. L.; Kruglyak, S.; Graige, M. S.; Garcia, F.; Kermani, B. G.; Zhao, C.; Che, D.; Dickinson, T.; Wickham, E.; Bierle, J.; Doucet, D.; Milewski, M.; Yang, R.; Siegmund, C.; Haas, J.; Zhou, L.; Oliphant, A.; Fan, J.-B.; Barnard, S.; Chee, M. S. *Genome Res.* **2004**, *14*, 870–877.
- (14) McGall, G. H.; Barone, A. D.; Diggelman, M.; Fodor, S. P. A.; Gentalen, E.; Ngo, N. *J. Am. Chem. Soc.* **1997**, *119*, 5081–5090.
- (15) Rennie, C.; Noyes, H. A.; Kemp, S. J.; Hulme, H.; Brass, A.; Hoyle, D. C. *BMC Genomics* **2008**, *9*, 317.
- (16) Affymetrix Genome Human SNP Nsp/Sty 6.0 user guide.
- (17) Epstein, J. R.; Lee, M.; Walt, D. R. *Anal. Chem.* **2002**, *74*, 1836–1840.
- (18) Fan, J.-B.; Gunderson, K. L.; Bibikova, M.; Yeakley, J. M.; Chen, J.; Wickham Garcia, E.; Lebruska, L. L.; Laurent, M.; Shen, R.; Barker, D. *Methods Enzymol.* **2006**, *410*, 57–73.
- (19) Fan, J.-B.; Hu, S. X.; Craumer, W. C.; Barker, D. L. *Biotechniques* **2005**, *39*, 583–588.
- (20) Michael, K. L.; Taylor, L. C.; Schultz, S. L.; Walt, D. R. *Anal. Chem.* **1998**, *70*, 1242–1248.
- (21) Dunning, M. J.; Smith, M. L.; Ritchie, M. E.; Tavare, S. *Bioinf.* **2007**, *23*, 2183–2184.
- (22) Kuhn, K.; Baker, S. C.; Chudin, E.; Lieu, M.-H.; Oeser, S.; Bennett, H.; Rigault, P.; Barker, D.; McDaniel, T. K.; Chee, M. S. *Genome Res.* **2004**, *14*, 2347–2356.
- (23) Pease, A. C.; Solas, D.; Sullivan, E. J.; Cronin, M. T.; Holmes, C. P.; Fodor, S. P. *A Proc. Natl. Acad. Sci. U.S.A.* **1994**, *91*, 5022–5026.
- (24) Gunderson, K. L. *Methods Mol. Biol.* **2009**, *529*, 197–213.
- (25) Gurtner, C.; Tu, E.; Jamshidi, N.; Haigis, R. W.; Onofrey, T. J.; Edman, C. F.; Sosnowski, R.; Wallace, B.; Heller, M. J. *Electrophoresis* **2002**, *23*, 1543–1550.
- (26) Heller, M. J.; Forster, A. H.; Tu, E. *Electrophoresis* **2000**, *21*, 157–164.
- (27) Sosnowski, R. G.; Tu, E.; Butler, W. F.; O'Connel, J. P.; Heller, M. J. *Proc. Natl. Acad. Sci. U.S.A.* **1997**, *94*, 1119–1123.
- (28) Livshits, M. A.; Mirzabekov, A. D. *Biophys. J.* **1996**, *71*, 2795–2801.
- (29) Edman, C. F.; Raymond, D. E.; Wu, D. J.; Tu, E.; Sosnowski, R. G.; Butler, W. F.; Nerenberg, M.; Heller, M. J. *Nucleic Acids Res.* **1997**, *25*, 4907–4914.
- (30) Kolchinsky, A.; Mirzabekov, A. *Hum. Mutat.* **2002**, *19*, 343–360.

- (31) Zangmeister, R. A.; Tarlov, M. J. *Anal. Chem.* **2004**, *76*, 3655–3659.
- (32) Emrich, C. A.; Tian, H.; Medintz, I. L.; Mathies, R. A. *Anal. Chem.* **2002**, *74*, 5076–5083.
- (33) Paegel, B. M.; Emrich, C. A.; Wedemayer, G. J.; Scherer, J. R.; Mathies, R. A. *Proc. Natl. Acad. Sci. U.S.A.* **2002**, *99*, 574–579.
- (34) Lagally, E. T.; Medintz, I. L.; Mathies, R. A. *Anal. Chem.* **2001**, *73*, 565–570.
- (35) Thaitrong, N.; Toriello, N. M.; Bueno, N. D.; Mathies, R. A. *Anal. Chem.* **2009**, *81*, 1371–1377.
- (36) Jensen, E. C.; Bhat, B. P.; Mathies, R. A. *Lab Chip* **2010**, *10*, 685–691.
- (37) Grover, W. H.; Skelley, A. M.; Liu, C. N.; Lagally, E. T.; Mathies, R. A. *Sens. Actuators, B* **2003**, *89*, 315–323.
- (38) Paegel, B. M.; Yeung, S. H. I.; Mathies, R. A. *Anal. Chem.* **2002**, *74*, 5092–5098.
- (39) Toriello, N. M.; Liu, C. N.; Blazej, R. G.; Thaitrong, N.; Mathies, R. A. *Anal. Chem.* **2007**, *79*, 8549–8556.
- (40) Emrich, C. A.; Medintz, I. L.; Chu, W. K.; Mathies, R. A. *Anal. Chem.* **2007**, *79*, 7360–7366.
- (41) Heo, J.; Crooks, R. M. *Anal. Chem.* **2005**, *77*, 6843–6851.
- (42) SantaLucia, J.; Hicks, D. *Annu. Rev. Biophys. Biomol. Struct.* **2004**, *33*, 415–440.
- (43) Wick, L. M.; Rouillard, J. M.; Whittam, T. S.; Gulari, E.; Tiedje, J. M.; Hasham, S. A. *Nucleic Acids Res.* **2006**, *34*, e26.
- (44) Gunnarsson, A.; Jonsson, P.; Zhdanov, V. P.; Hook, F. *Nucleic Acids Res.* **2009**, *37*, e99.
- (45) Tawa, K.; Knoll, W. *Nucleic Acids Res.* **2004**, *32*, 2372–2377.
- (46) Ikuta, S.; Takagi, K.; Bruce Wallace, R.; Itakura, K. *Nucleic Acids Res.* **1987**, *15*, 797–811.
- (47) Naiser, T.; Kayser, J.; Michel, W.; Mai, T.; Ott, A. *BMC Bioinf.* **2008**, *9*, 509.
- (48) Stimpson, D. I.; Hoijer, J. V.; Hsieh, W. T.; Jou, C.; Gordon, J.; Theriault, T.; Gamble, R.; Baldeschwieler, J. D. *Proc. Natl. Acad. Sci. U.S.A.* **1995**, *92*, 6379–6383.
- (49) Sorokin, N. V.; Chechetkin, V. R.; Pan'kov, S. V.; Somova, O. G.; Livshits, M. A.; Donnikov, M. Y.; Turygin, A. Y.; Barsky, V. E.; Zasedatelev, A. S. *J. Biomol. Struct. Dyn.* **2006**, *24*, 57–66.
- (50) Lee, S. H.; Walker, D. R.; Cregan, P. B.; Boerma, H. R. *Theor. Appl. Genet.* **2004**, *110*, 167–74.

■ NOTE ADDED AFTER ASAP PUBLICATION

This paper was published on the Web on December 30, 2011. Corrections were made that include some minor text changes, addition of a footnote to Table 1, and changes to the references, and the corrected version was reposted on January 5, 2012.